Supporting Information

Tailoring light emission properties, optoelectronic and optothermal responses from rare earth-doped bismuth oxide for multifunctional light shielding, temperature sensing and photodetector

Liumin Fan[a], Yang Li[a,b,*], Xiaohui Lin[a], Junhao Peng[a], Guifang Ju[a], Shaoan Zhang[a,d], Li Chen[a], Fupo He[c], Yihua Hu[a,*]

[a] *School of Physics and Optoelectronic Engineering, Guangdong University of Technology, Guangzhou 510006, China.*

[b] *State Key Laboratory of Luminescent Materials and Devices, South China University of Technology, Guangzhou 510640, China.*

[c] *School of Electromechanical Engineering, Guangdong University of Technology, Guangzhou 510006, China.*

[d] *Guangzhou Maritime University, Guangzhou 510006, China.*

Corresponding authors: huyh@gdut.edu.cn; lychris@sina.com

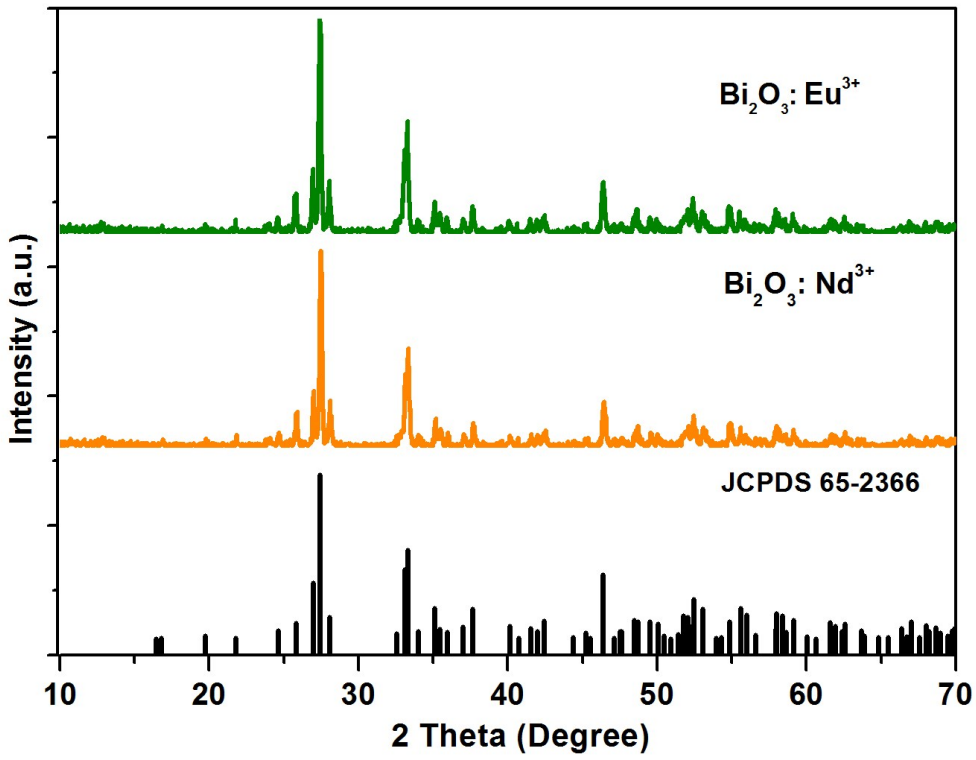

Figure S1: The XRD patterns of Bi_2O_3 and Bi_2O_3: Re^{3+} (Re^{3+} = Nd^{3+}, Eu^{3+}) with PDF card of Bi_2O_3.

The phases of the as prepared are first explored by XRD analysis and the results are shown in Figure S1. The acquired XRD pattern of Bi_2O_3: Re^{3+} (Re^{3+} = Nd^{3+}, Eu^{3+}) are similar to that of the pure Bi_2O_3 and all the diffraction peaks of pure Bi_2O_3 and Bi_2O_3: Re^{3+} (Re^{3+} = Nd^{3+}, Eu^{3+}) sample are well indexed to JCPDS no. 65–2366. Further, no other impurity phases are observed in pure Bi_2O_3 and Bi_2O_3: Re^{3+} (Re^{3+} = Nd^{3+}, Eu^{3+}) samples，indicating that the pure α-Bi_2O_3 are successfully synthesized as host' material and the dopants had no significant influence on the hosts' lattice.

Figure 2a, S2 shows the calculated band structure of Bi_2O_3 and Bi_2O_3: Sm^{3+}, respectively. Structure relaxations and properties calculations are performed using density functional theory (DFT)[1] within the generalized gradient approximation (GGA)[2] as implemented in the VASP code[3]. Energy convergence precision and the plane wave kinetic energy cutoff are set to 10^{-5} eV and 500eV. We sample the Brillouin zone with uniform Γ-centered meshes of 2π*0.05 $Å^{-1}$(4x3x3) for structure relaxations and 2π * 0.03 $Å^{-1}$(7x5x5) for properties calculations. The band-gap energy of Bi_2O_3: Sm^{3+} is obtained (1.6 eV, Figure S2) through the theoretical calculation. And,

the experimental diffuse reflectance of the Bi_2O_3: Sm^{3+} sample is turn into a Kubelka–Munk function F(R) in Figure S3. As an approximation, we can read the value of band-gap energy in Bi_2O_3: Sm^{3+} sample is 2.42 eV. Analogously, the experimental value of band-gap energy of Bi_2O_3 sample is in agreement with our theoretical calculation.

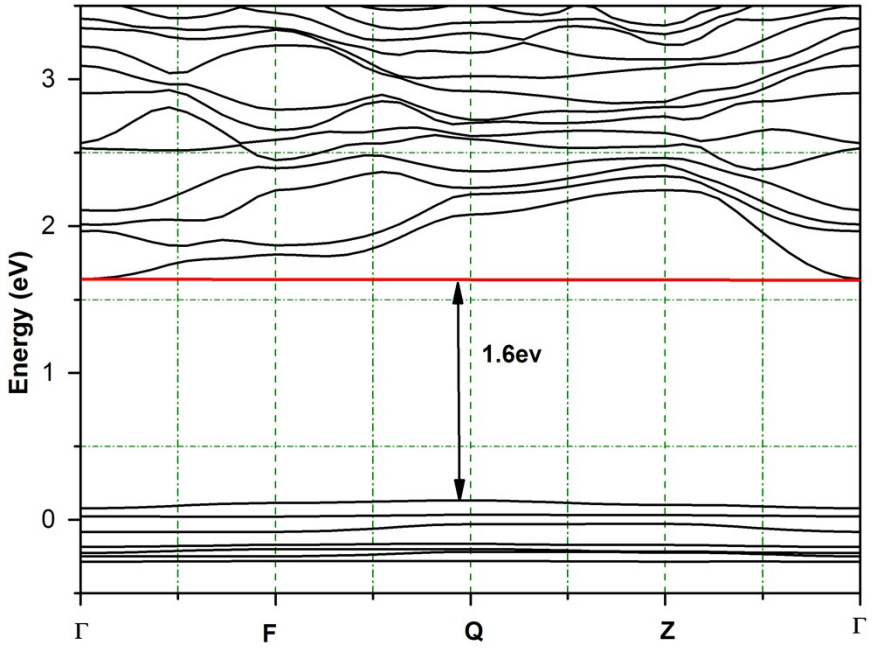

Figure S2: The Calculated band structure for Bi_2O_3: Sm^{3+}.

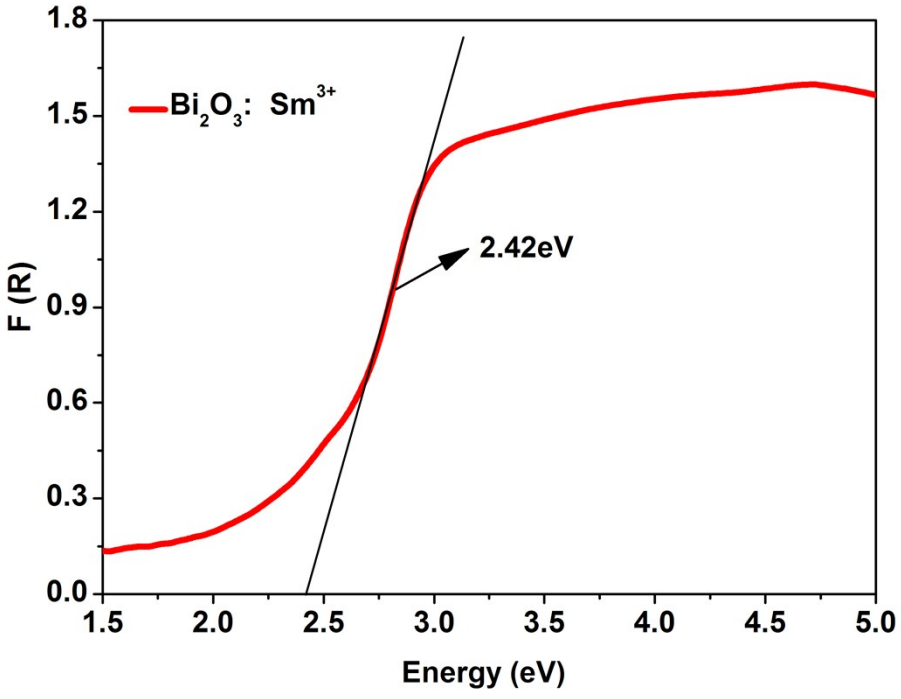

Figure S3: Experimental diffuse reflectance is turn into a Kubelka–Munk function F(R). $(hvF(R))^{1/2}$–hv plot of the of the Bi_2O_3: Sm^{3+}. The bandgap energy is estimated from the intercept of a fitted straight line (black).

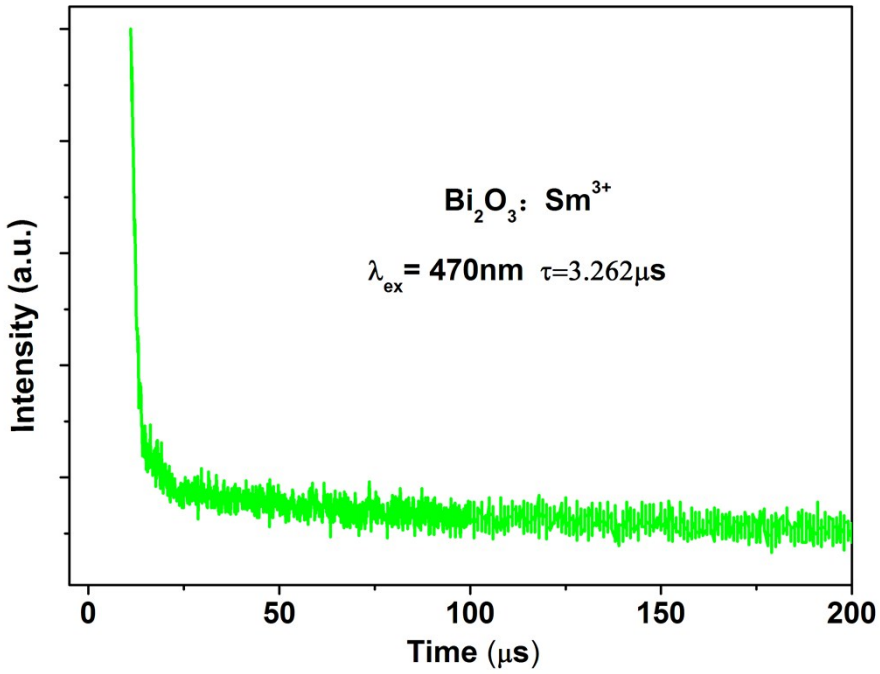

Figure S4: Decay curves of Bi_2O_3: Sm^{3+} phosphor (excited at 470 nm, and monitored at 653nm).

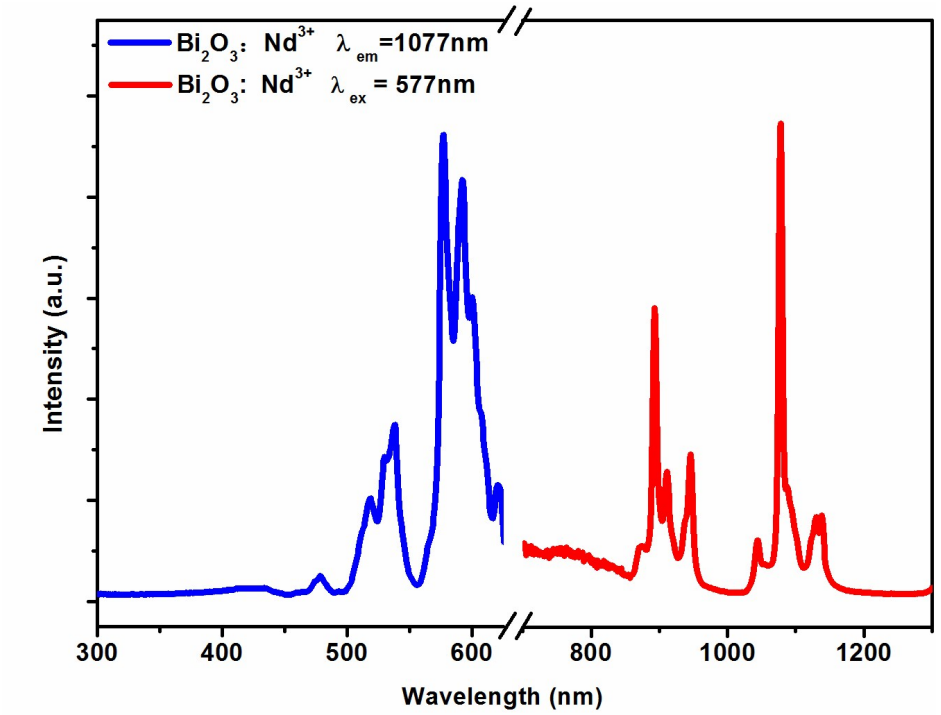

Figure S5: PLE (left) and PL (right) spectra of Bi_2O_3: Nd^{3+} phosphor.

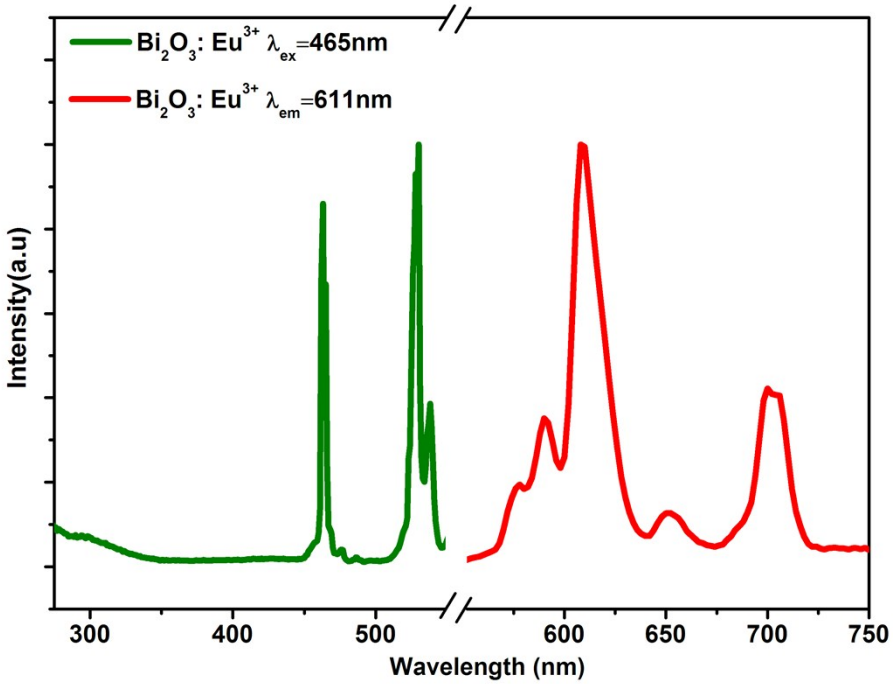

Figure S6. PLE (left) and PL (right) spectra of Bi_2O_3: Eu^{3+} phosphor.

The PLE and PL spectra of Bi_2O_3: Re^{3+} (Re^{3+} =Nd^{3+}, Eu^{3+}) are shown in Figure S5, S6. From Figure S5, we can see that the PLE spectra of Bi_2O_3: Nd^{3+} contains a series of excitation monitored at 1077 nm peaks at 577 nm and 536 nm, which are assigned to the $^4I_{9/2} \rightarrow {}^4G_{5/2}$, $^4I_{9/2} \rightarrow {}^4G_{7/2}$ transitions of the Nd^{3+} ions, respectively. And, the emission spectra is constitute of many typical emission bands centered at 1077 nm and 890 nm under 577nm excitation, which can be ascribed to the electronic transitions of Nd^{3+} from $^4F_{3/2}$ to $^4I_{11/2}$, $^4H_{9/2}$, respectively. Furthermore, from Figure S6, we should note that the 465 nm and 529 nm excitation bands in Bi_2O_3: Eu^{3+} originate from the $^7F_0 \rightarrow {}^5D_2$, $^7F_0 \rightarrow {}^5D_1$ transition in PLE spectra. the band at 611 nm and 700 nm should be assigned to the $^5D_0 \rightarrow {}^7F_2$, $^5D_0 \rightarrow {}^7F_4$ transitions of Eu^{3+} ions in PL spectra. All the investigation about PL and PLE spectra can be well according with our theoretical conjecture.

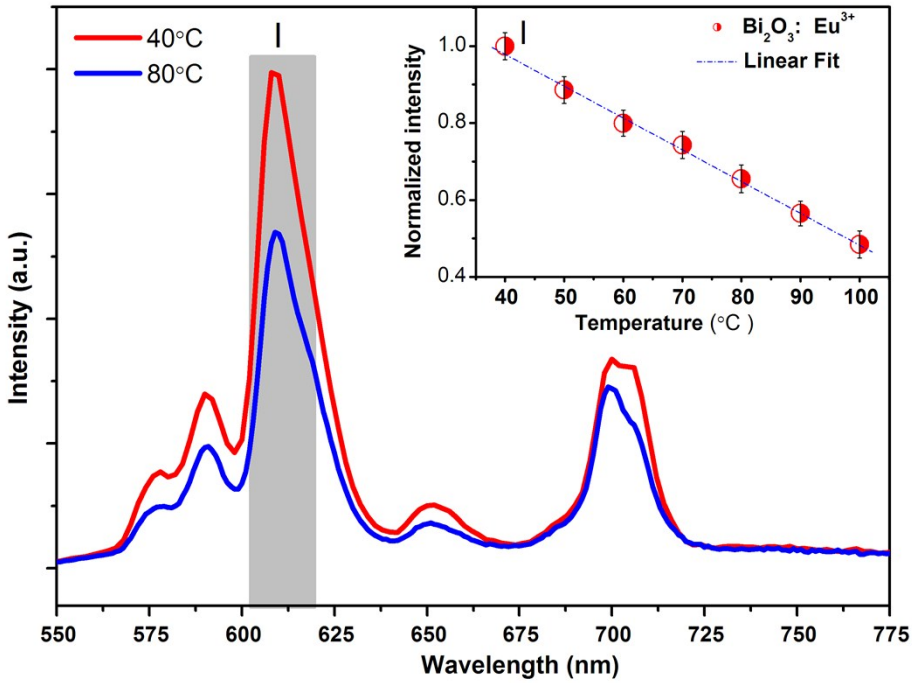

Figure S7: Temperature-dependent emission spectrum of Bi_2O_3: Eu^{3+}. The inset shows the variation of intensity (I) as a function of the temperature.

A monolog plot of the normalized PL emission intensity (I) at 611nm as a function of temperature in the range of 40–100°C is shown in Figure S7(a). We find that the luminescence intensity changes linearly with temperature with excellent temperature sensitivity (0.8% $°C^{-1}$).

The stable I–V curve of Bi_2O_3: Nd^{3+} bias on 30 V is shown in Figure S8(a), which are excited with the light of different wavelength (254, 460 and 590 nm) under the same measurement condition. And, the peak of current sample at a bias of 30 V is plotted as a function of wavelength is shown as in Figure 5c. Further, the dark current (~0.205 µA) is found to be lowest and an abrupt increase in the current is observed. Apparently, the current corresponding to 254, 460 and 590 nm wavelength reached ~ 0.254, ~ 0.229 and ~ 0.329 µA.

The thermal sensitivity resulting from temperature dependence of the intensity can be calculated by

$$S = dI/dT \qquad (1)$$

where S denotes the thermal sensitivity, I denotes the intensity of emission band at

653 nm and T denotes the temperature of the samples (°C).

Further, the thermal sensitivity resulting from spectra shift can be calculated by

$$S = d(\Delta\lambda)/dT \qquad (2)$$

where S denotes the thehermal sensitivity, $\Delta\lambda$ denotes the D-value of spectral shift (nm), T denotes the temperature of the samples (°C).

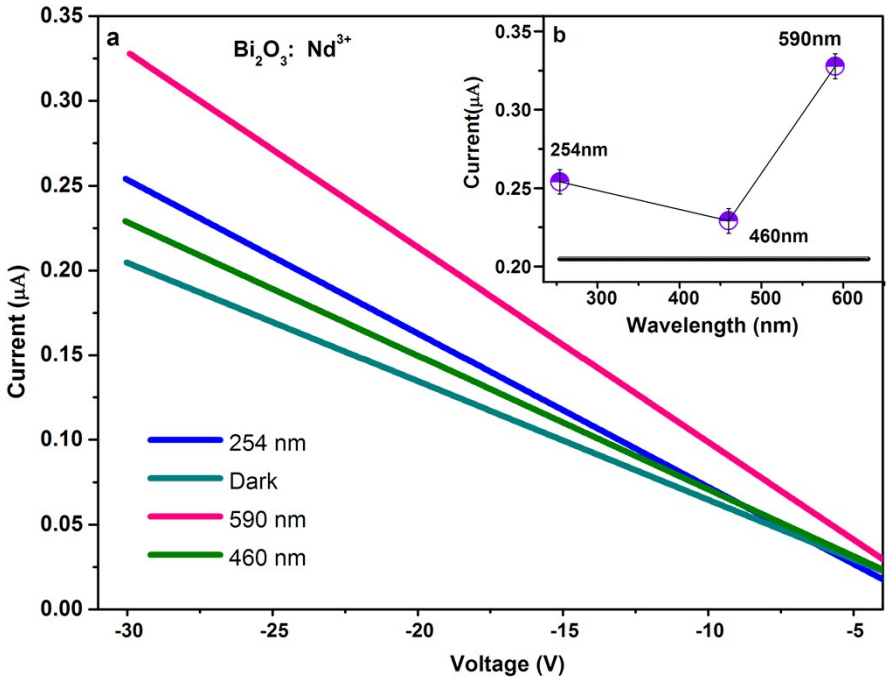

Figure S8: The optoelectronic performance of Bi_2O_3: Nd^{3+} phosphor (a) The current response under dark, 254, 460, and 590 nm excitation of Bi_2O_3: Nd^{3+}. (b) The inset shows the variation of current with increasing illumination wavelength.

References

1. P. E. Blöchl, *Phys. Rev.*, 1994, B50, 17953–17979.
2. J. P. Perdew, K Burke and M. Ernzerhof, *Phys. Rev. Lett.*, 1996, 77, 3865–3868.
3. G. Kresse and J. Furthmüller, *Phys. Rev. B*, 1996, 54, 11169–11186.